Enhancing Isoprene Polymerization with high Activity and Adjustable Monomer Enchainment using Cyclooctyl-Fused Iminopyridine Iron Preatalysts

Nighat Yousuf[a,b,c], Yanping Ma[a,*], Qaiser Mahmood[b,*], Wenjuan Zhang[d,*], Yizhou Wang[a,c], Hassan Saeed[a,b,c], Wen-Hua Sun[a,b,c,*]

[a]Key Laboratory of Engineering Plastics and Beijing National Laboratory for Molecular Science, Institute of Chemistry, Chinese Academy of Sciences, Beijing 100190, China. E-mail: myanping@iccas.ac.cn, whsun@iccas.ac.cn;

[b]Chemistry and Chemical Engineering Guangdong Laboratory, Shantou 515031, China. E-mail: qaiser@ccelab.com.cn

[c]CAS Research/Education Center for Excellence in Molecular Sciences and International School, University of Chinese Academy of Sciences, Beijing 100049, China

[d]Beijing Key Laboratory of Clothing Materials R&D and Assessment, School of Materials Science and Engineering, Beijing Institute of Fashion Technology, Beijing 100029, China. E-mail: zhangwj@bift.edu.cn

Table of contents

General consideration and materials

The synthesis of iron catalysts and the isoprene polymerization process were typically carried out under an inert atmosphere of dry argon using standard Schlenk techniques. Toluene was dried using sodium metal, and all other solvents were subjected to reflux over CaH_2 under an argon atmosphere before use. The co-catalysts, namely $AlMe_2Cl$ (0.9 M in heptane), and $AlEt_2Cl$ (2.0 M in hexane), and MAO (1.67 M in toluene), were purchased from Shanghai Macklin Biochemical Co. Ltd. and Anhui Botai Electronic Materials Co. and were used as received without any further modifications. Analytical grade isoprene was purchased and subjected to purification by distillation over CaH_2 under an argon atmosphere, after which it was stored at low temperature. All other commercially available chemicals were used without the need for additional purification. ^1H and ^{13}C NMR measurements were performed using a Bruker Avance Neo 600 MHz spectrometer, with deuterated chloroform ($CDCl_3$) as the internal standard and tetramethylsilane (TMS) as the internal reference. Chemical shifts are reported in ppm, while *J* values in Hz. Fourier transform infrared (FT-IR) analysis was performed using a Bruker Tensor II FT-IR spectrometer. The elemental analysis of iron complexes (**Fe^{H}-$Fe^{2Et,Me}$**) was determined using a Thermoscientific Flashsmart instrument micro-analyzer. Gel permeation chromatography (GPC) was conducted using a PL-GPC50 instrument and 1260 Infinity II High Temperature GPC System equipped with a refractive index detector. The GPC system utilized mixed columns with a combined length of 650 and an internal diameter of 7.5 mm. The samples were dissolved in tetrahydrofuran (THF) and 1,2,4-trichlorobenzene (TCB) at a temperature of 40 ℃ and 120 ℃, respectively and elution of THF/TCB occurred at a flow rate of 1.0 ml/min. The columns were calibrated using standard polystyrene samples.

Procedure for isoprene polymerization

Isoprene polymerization was conducted using a Schlenk technique under argon atmosphere. The precatalysts such as **Fe^{H}** (5 μmol), and toluene (5 ml) were added sequentially into the schlenk flask, then required amount of MAO was added, stirred for 1 minute at the desired temperature and then immediately isoprene (2 ml) was added into the solution. After the desired reaction time, the polymerization was quenched with 10% hydrochloric acid in ethanol. The polymer was washed with

excess of ethanol three times, filtered and then dried under vacuum at room temperature to constant weight.

X-Ray Crystallographic Studies

Single crystals of **Fe^{H}**, **Fe^{2Me}** and **Fe^{2Et,Me}**, suitable for X-ray determinations, were grown through the slow diffusion of n-hexane into a solution of the corresponding complexes in dichloromethane at room temperature. Single crystal X-ray diffraction analysis of **Fe^{H}, Fe^{2Me}** and **Fe^{2Et,Me}** was carried out using a Rigaku Sealed Tube CCD (Saturn 724+) diffractometer. This diffractometer utilized graphite-monochromated Cu-Kα radiation with a wavelength (λ) of 1.54184 Å. The measurements were conducted at a temperature of 169.98 (±10) K. The determination of cell parameters involved the global refinement of the positions of all collected reflections. Intensities obtained from the X-ray diffraction analysis were corrected for Lorentz and polymerization effects, and an empirical absorption correction was applied.

The structure of complex **Fe^{H}, Fe^{2Me}** and **Fe^{2Et,Me}** was solved using direct methods and subsequently refined through full-matrix least squares fitting on **Fe^{H}, Fe^{2Me}** and **Fe^{2Et,Me}**. Non-hydrogen atoms in each complex were refined anisotropically, while the positions of all hydrogen atoms were determined based on calculated positions. Data collected during the analysis were processed using the Olex2 program [1]. The solvent molecules, which do not influence the geometry of the main compound, were also solved. The crystal data and processing parameters for **Fe^{H}, Fe^{2Me}** and **Fe^{2Et,Me}** are presented in Table S1.

Table S1. Crystal data and structure refinement for **Fe^{H}, Fe^{2Me}** and **Fe^{2Et,Me}**

Identification code	**Fe^{H}**	**Fe^{2Me}**	**Fe^{2Et,Me}**
Empirical formula	$C_{102}H_{108}Cl_{13}Fe_5N_{12}$[+solvent]	$C_{38}H_{44}Cl_5Fe_2N_4$	$C_{44}H_{56}Cl_5Fe_2N_4$
Formula weight	2242.10	845.72	929.87
Temperature/K	169.99(10)	169.98(10)	169.98(10)
Crystal system	trigonal	triclinic	monoclinic
Space group	P3	P-1	$P2_1/c$
a/Å	12.4440(5)	9.9529(3)	18.1364(2)
b/Å	12.4440(5)	13.3706(4)	17.4597(2)
c/Å	20.0425(14)	15.0002(3)	14.3755(2)
α/°	90	86.305(2)	90
β/°	90	79.243(2)	99.2860(10)
γ/°	120	89.108(2)	90
Volume/Å^3	2687.9(3)	1957.00(9)	4492.44(10)
Z	1	2	4
ρ_{calc}g/cm^3	1.385	1.435	1.375
μ/mm^{-1}	8.648	9.334	8.181
F(000)	1155.0	874.0	1940.0

Crystal size/mm^3	0.3 × 0.25 × 0.2	0.3 × 0.25 × 0.2	0.28 × 0.25 × 0.2
Radiation	Cu Kα (λ = 1.54184)	Cu Kα (λ = 1.54184)	Cu Kα (λ = 1.54184)
2Θ range for data collection/°	4.408 to 154.708	6.01 to 152.068	4.938 to 155.34
Index ranges	-15 ≤ h ≤ 15, -15 ≤ k ≤ 14, -23 ≤ l ≤ 24	-10 ≤ h ≤ 12, -16 ≤ k ≤ 16, -18 ≤ l ≤ 18	-22 ≤ h ≤ 20, -21 ≤ k ≤ 19, -17 ≤ l ≤ 18
Reflections collected	10315	26005	36748
Independent reflections	5957 [R_{int} = 0.0479, R_{sigma} = 0.0650]	7859 [R_{int} = 0.0398, R_{sigma} = 0.0344]	9243 [R_{int} = 0.0350, R_{sigma} = 0.0300]
Data/restraints/parameters	5957/43/413	7859/2/447	9243/25/533
Goodness-of-fit on F^2	1.102	1.034	1.030
Final R indexes [I>=2σ (I)]	R_1 = 0.0502, wR_2 = 0.1350	R_1 = 0.0374, wR_2 = 0.0978	R_1 = 0.0396, wR_2 = 0.1006
Final R indexes [all data]	R_1 = 0.0679, wR_2 = 0.1450	R_1 = 0.0410, wR_2 = 0.0998	R_1 = 0.0458, wR_2 = 0.1043
Largest diff. peak/hole / e Å^{-3}	0.49/-0.36	0.58/-0.47	0.67/-0.40

^{1}H and ^{13}C NMR spectra for polyisoprenes

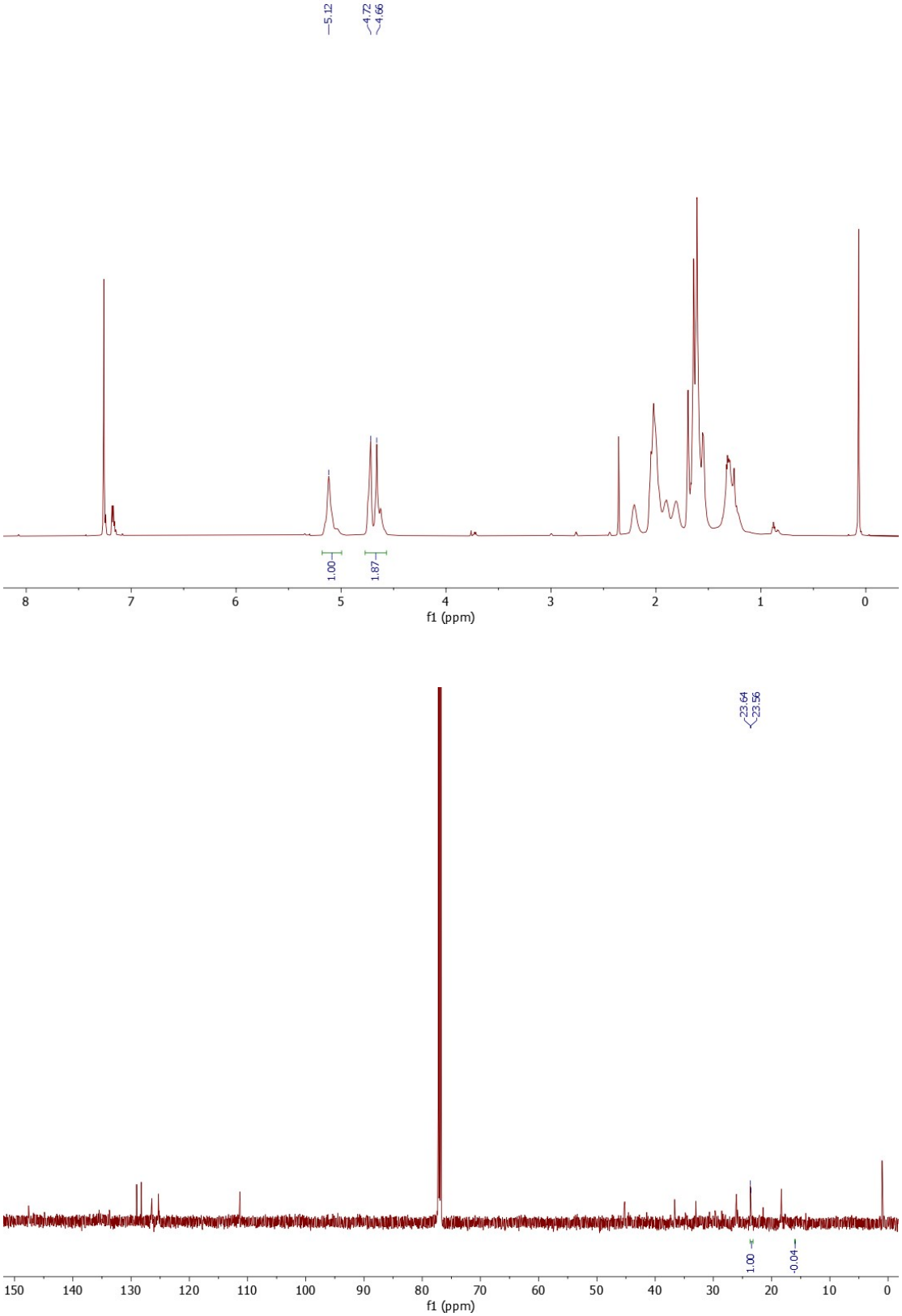

Figure S1. ^{1}H and ^{13}C NMR spectra of the polyisoprene obtained using **Fe^{H}**/MAO (Table 1, entry 3).

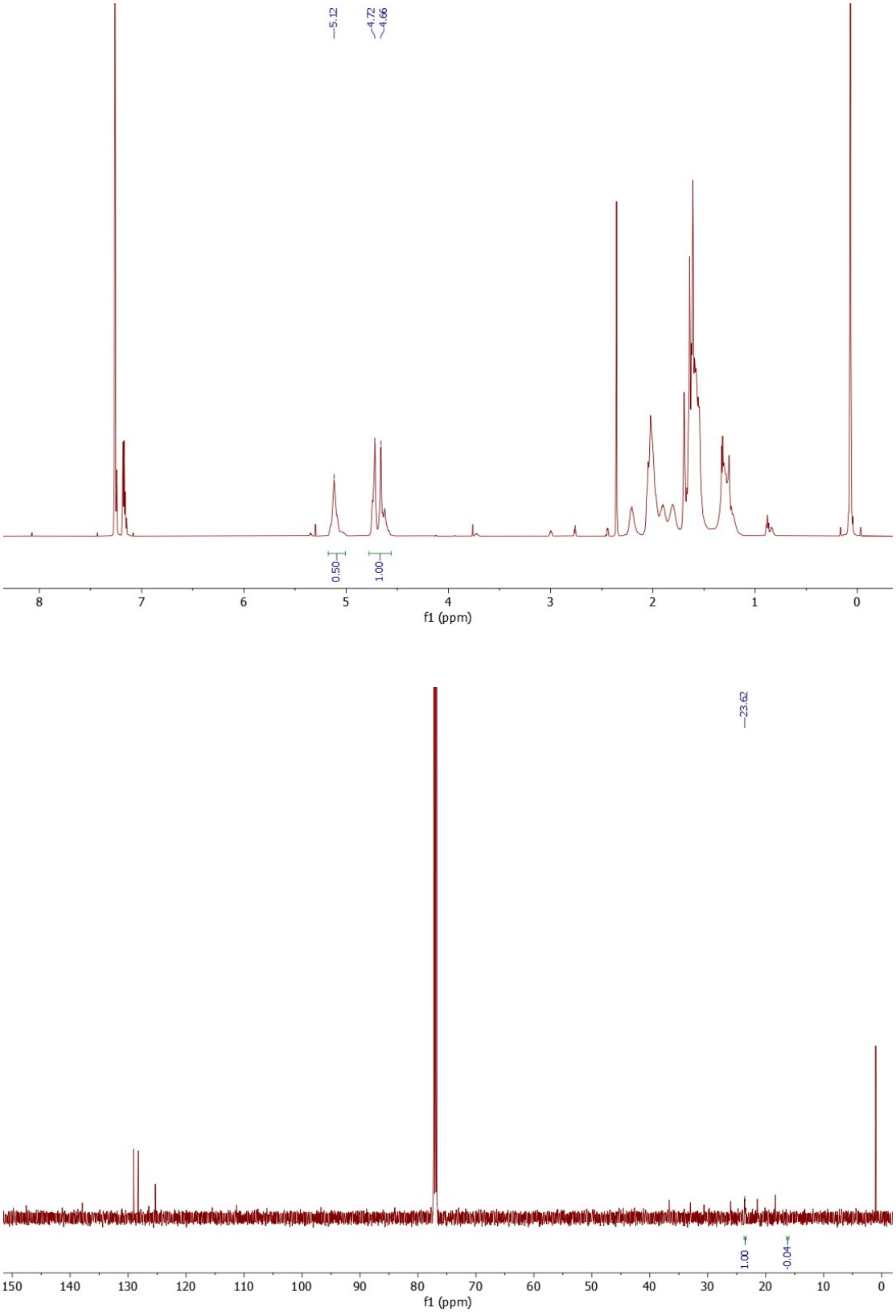

Figure S2. ^{1}H and ^{13}C NMR spectra of the polyisoprene obtained using $\mathbf{Fe^{H}}$/MAO (Table 2, entry 2).

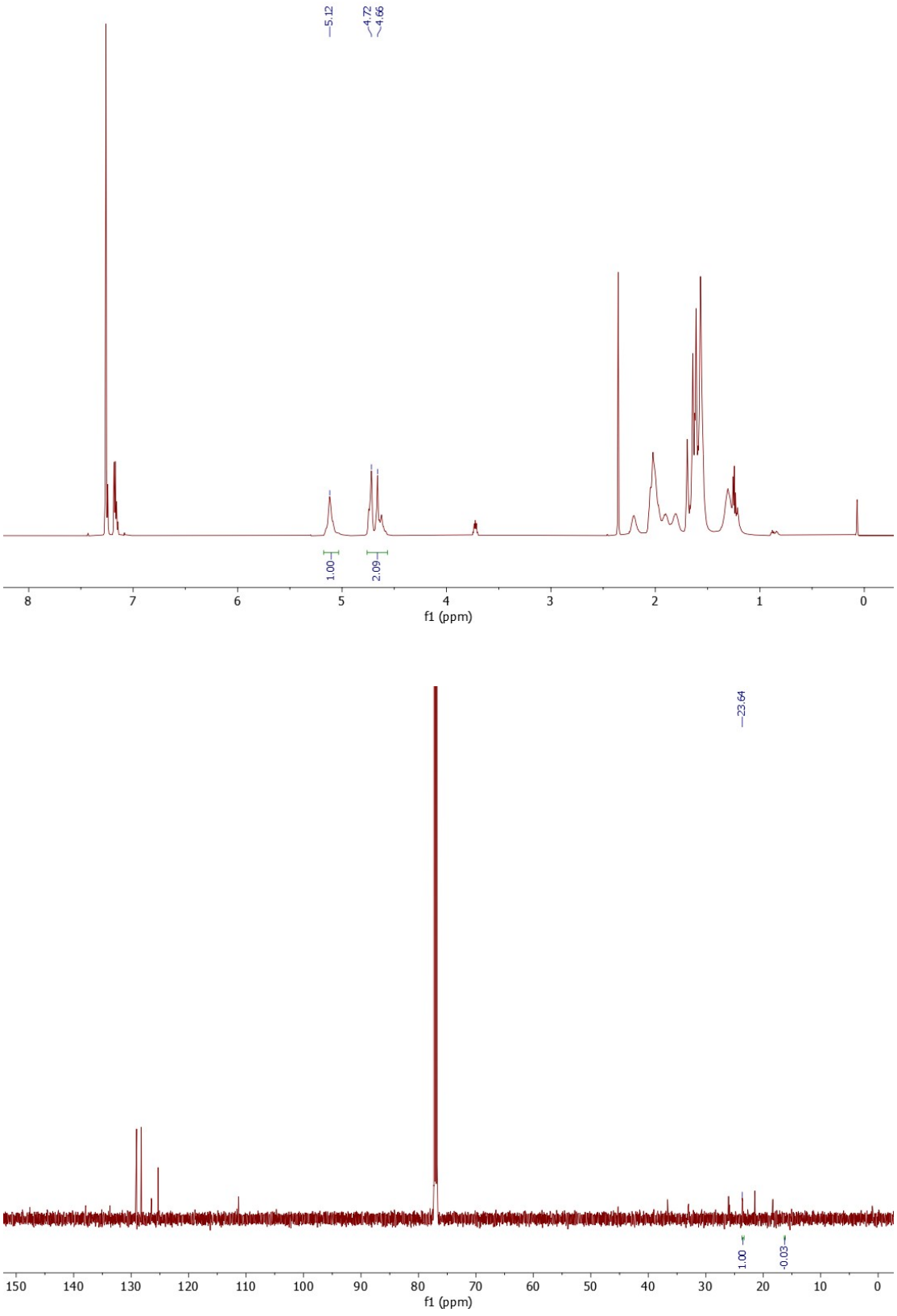

Figure S3. ^{1}H and ^{13}C NMR spectra of the polyisoprene obtained using $\mathbf{Fe^{H}}$/MAO (Table 2, entry 3).

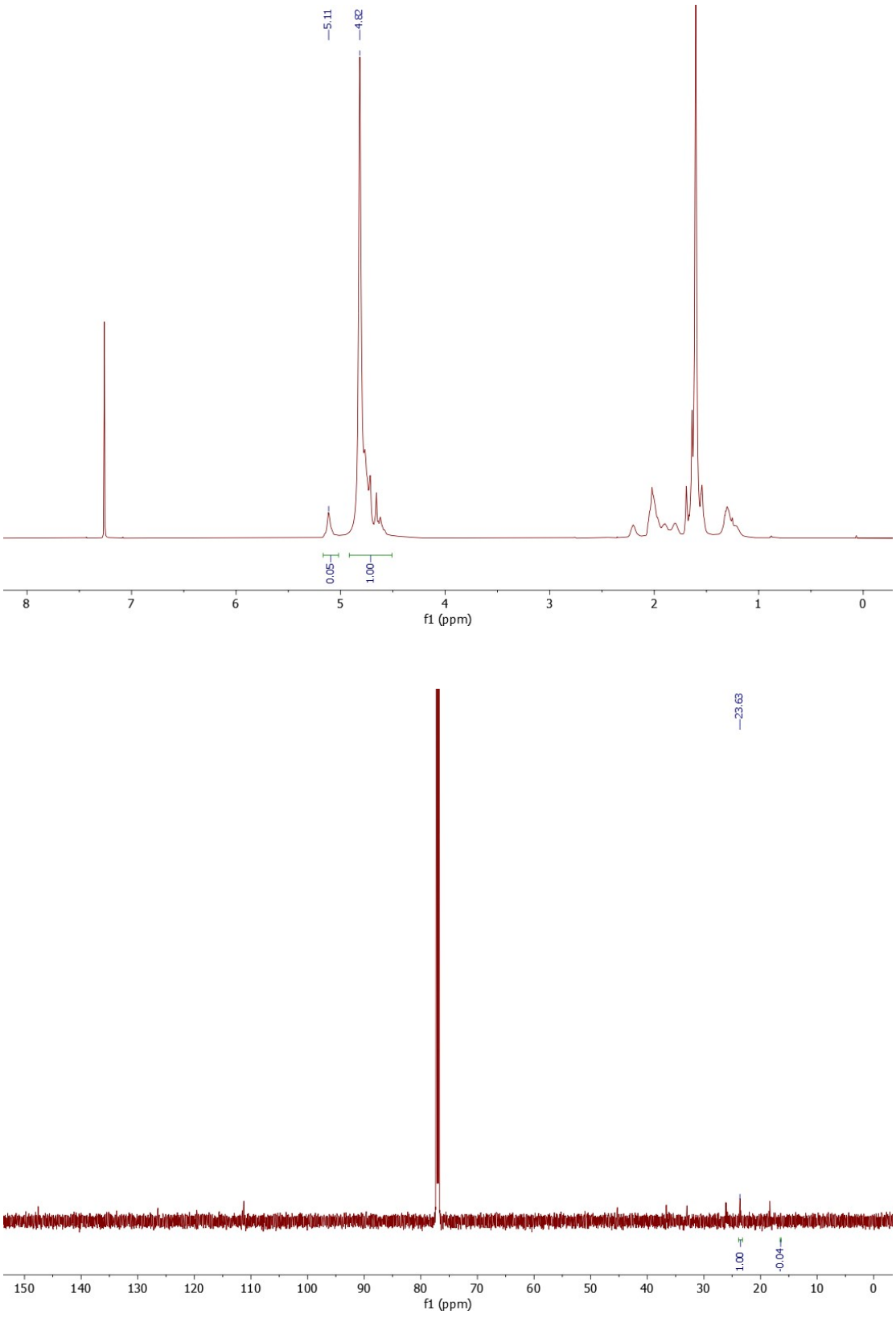

Figure S4. ^{1}H and ^{13}C NMR spectra of the polyisoprene obtained using $\mathbf{Fe^{H}}$/MAO (Table 2, entry 4).

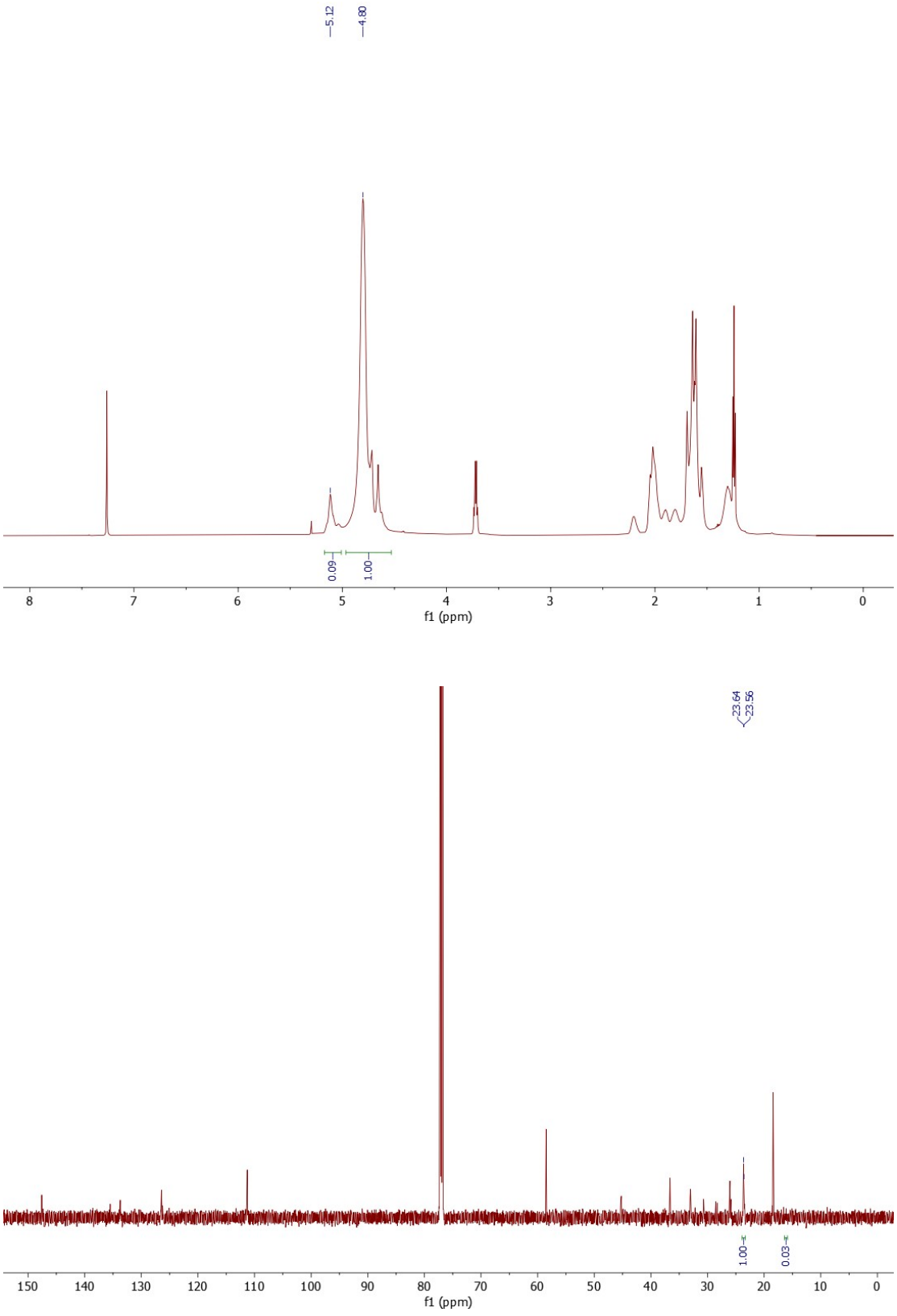

Figure S5. ^{1}H and ^{13}C NMR spectra of the polyisoprene obtained using **Fe^{H}**/MAO (Table 2, entry 5).

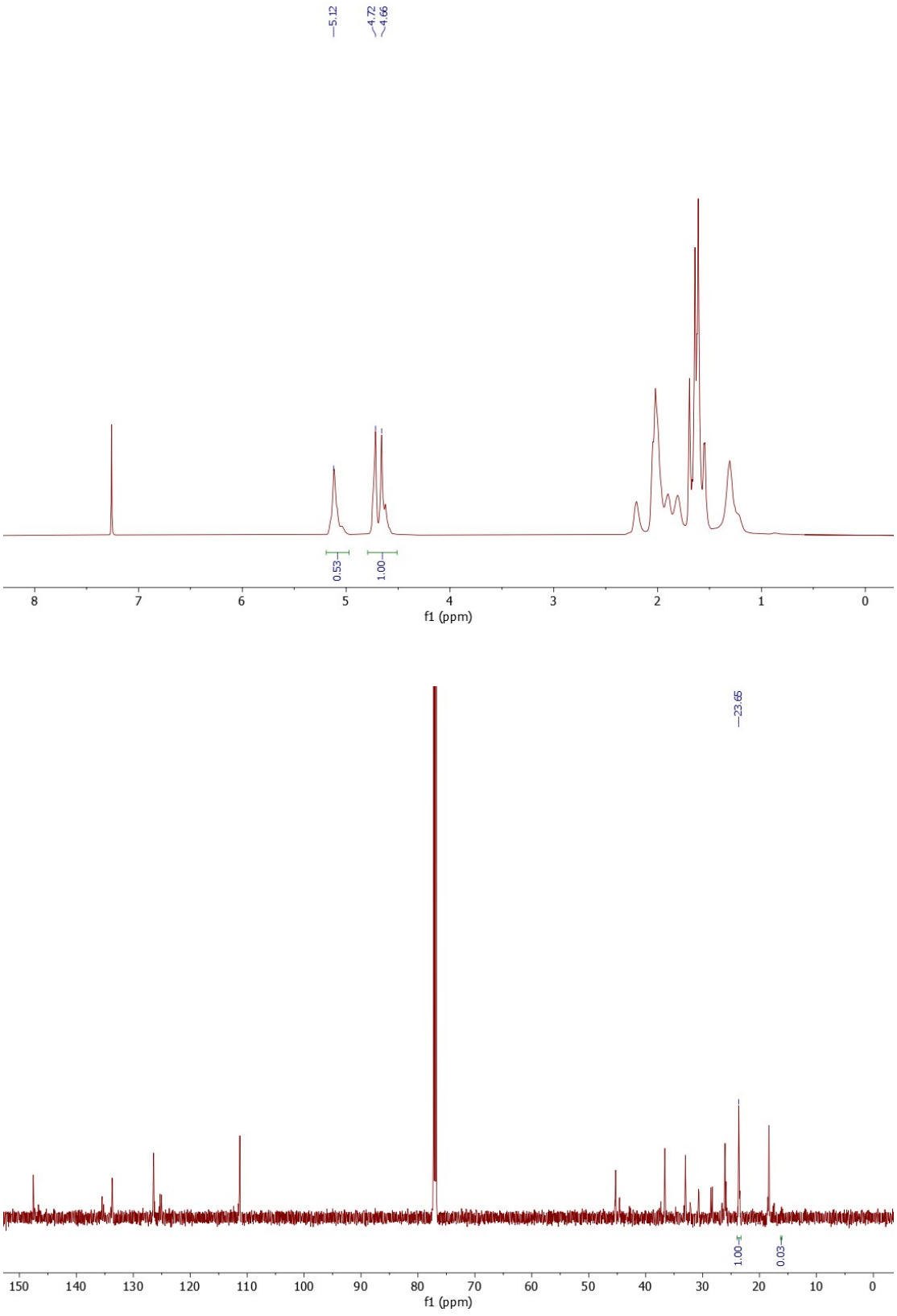

Figure S6. ^{1}H and ^{13}C NMR spectra of the polyisoprene obtained using **Fe^{H}**/MAO (Table 2, entry 6).

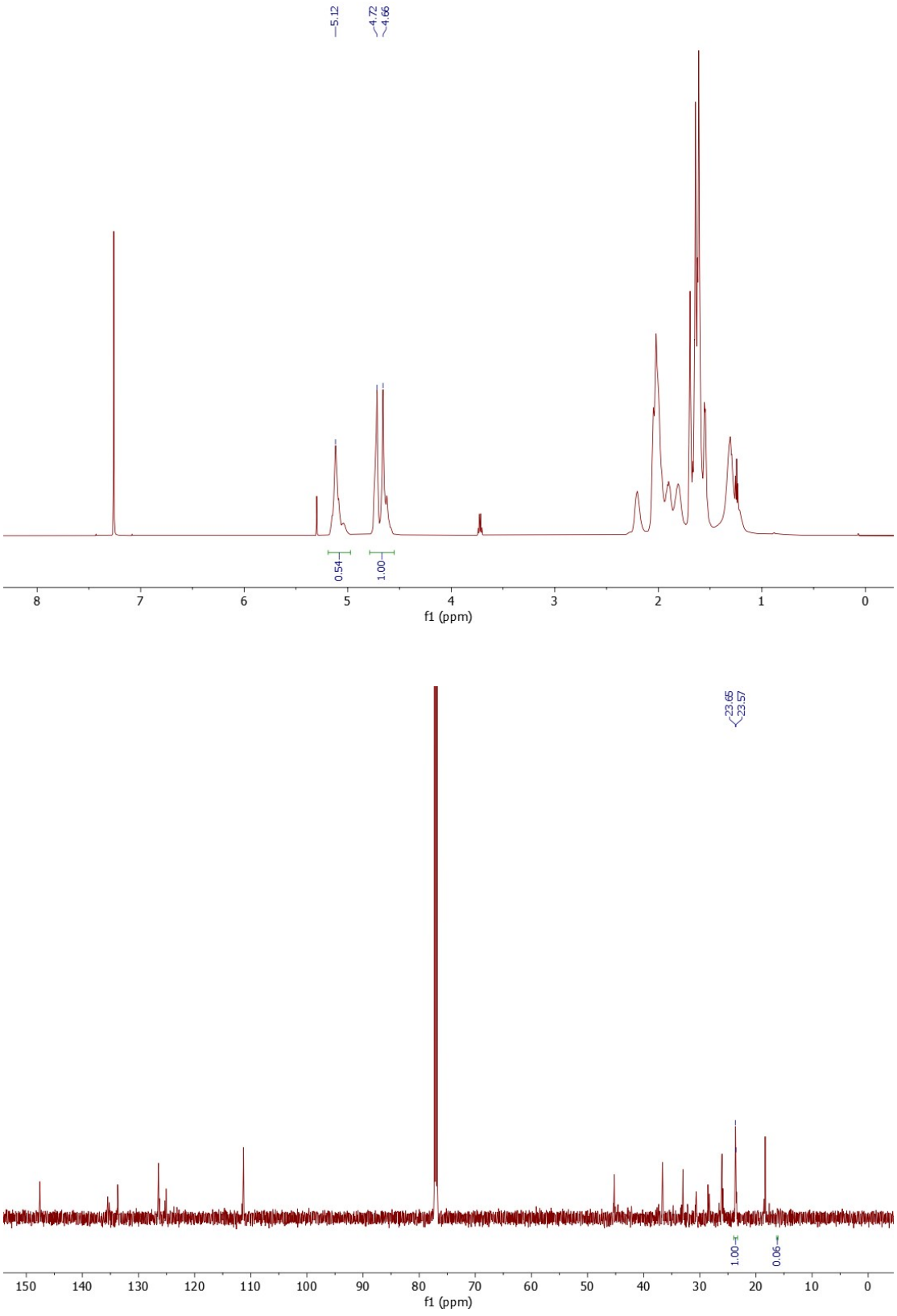

Figure S7. ^{1}H and ^{13}C NMR spectra of the polyisoprene obtained using **Fe^{H}**/MAO (Table 2, entry 7).

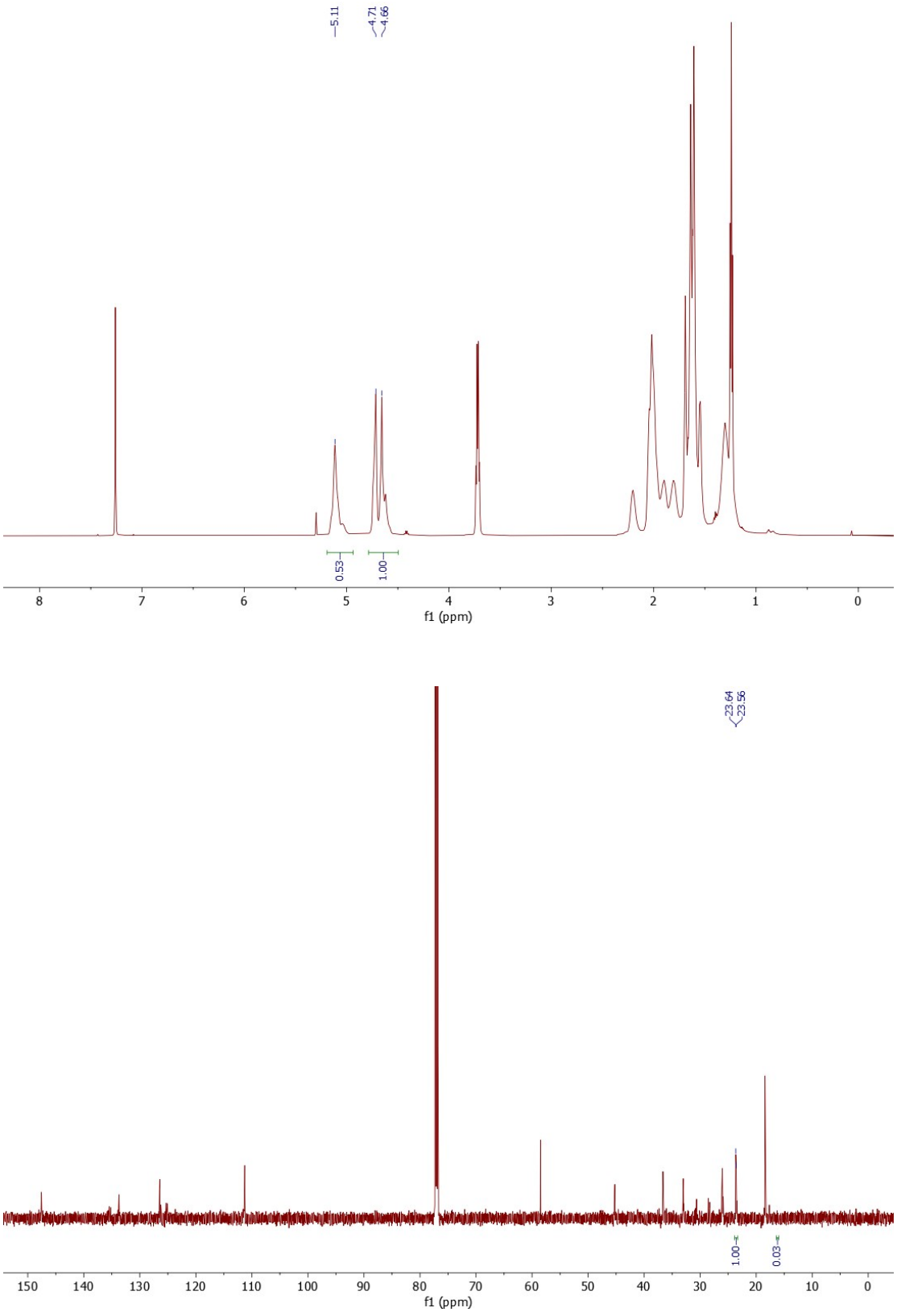

Figure S8. ^{1}H and ^{13}C NMR spectra of the polyisoprene obtained using **Fe^{H}**/MAO (Table 2, entry 8).

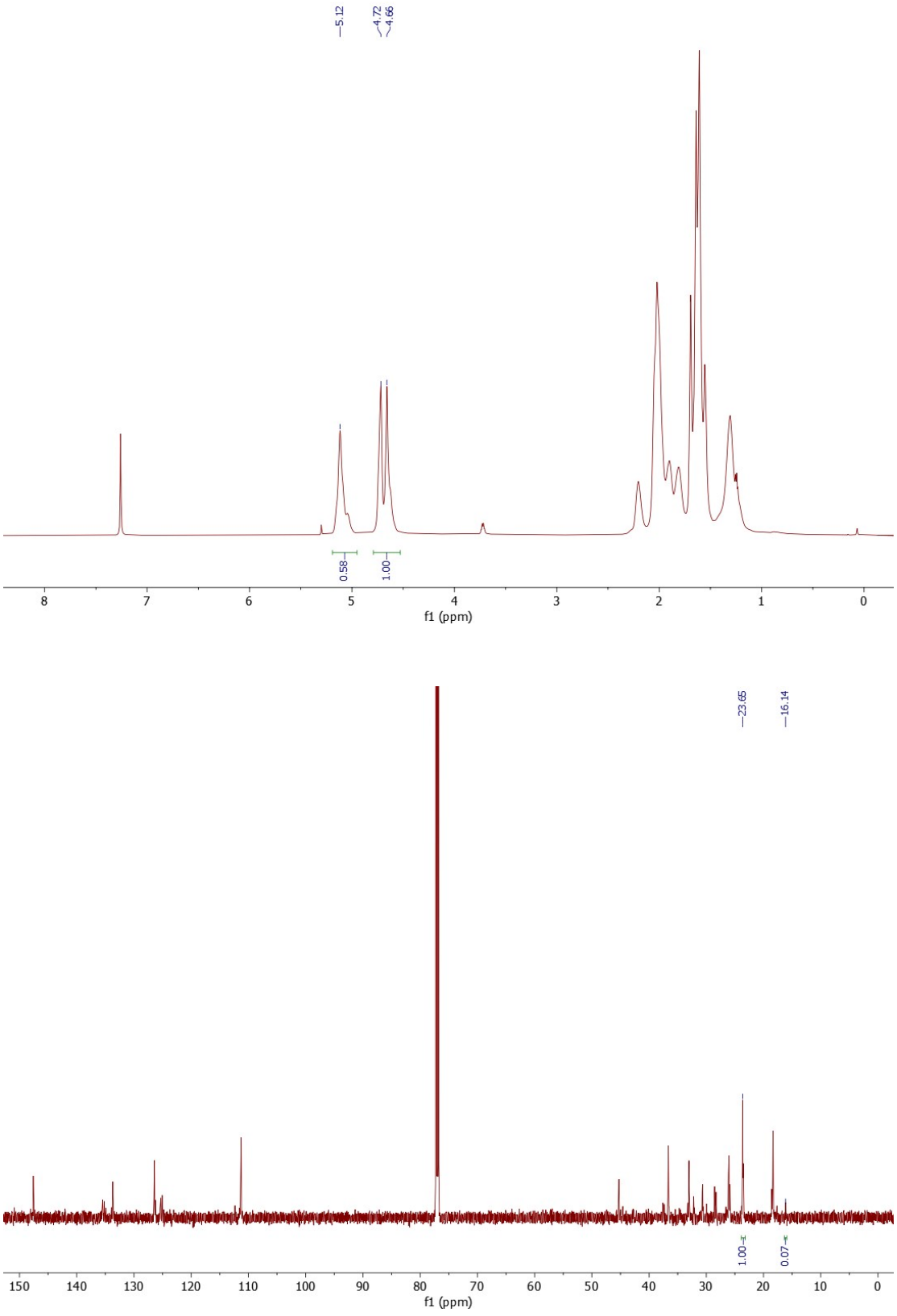

Figure S9. ^{1}H and ^{13}C NMR spectra of the polyisoprene obtained using **Fe^{H}**/MAO (Table 2, entry 9).

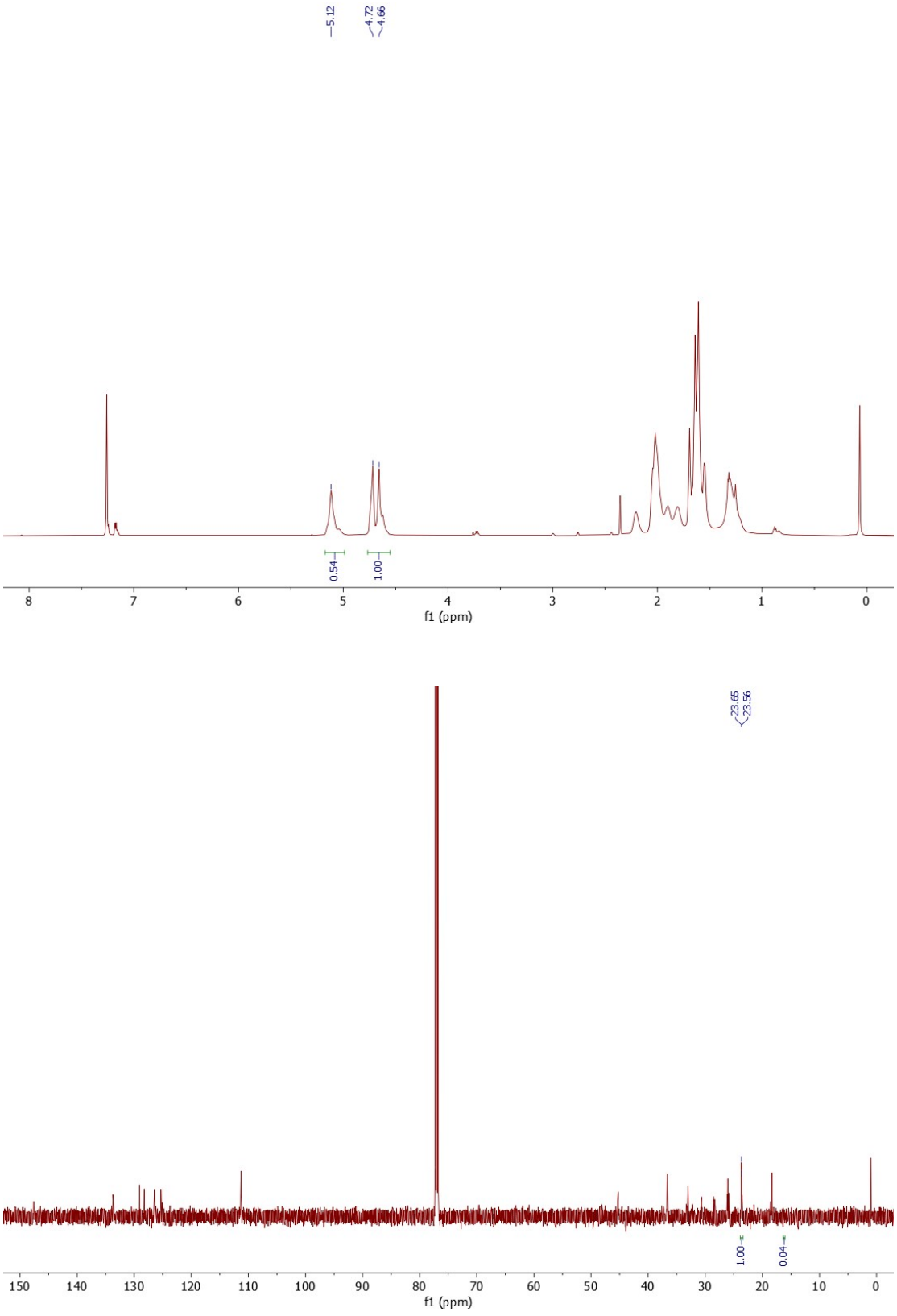

Figure S10. ^{1}H and ^{13}C NMR spectra of the polyisoprene obtained using **Fe^{H}**/MAO (Table 2, entry 10).

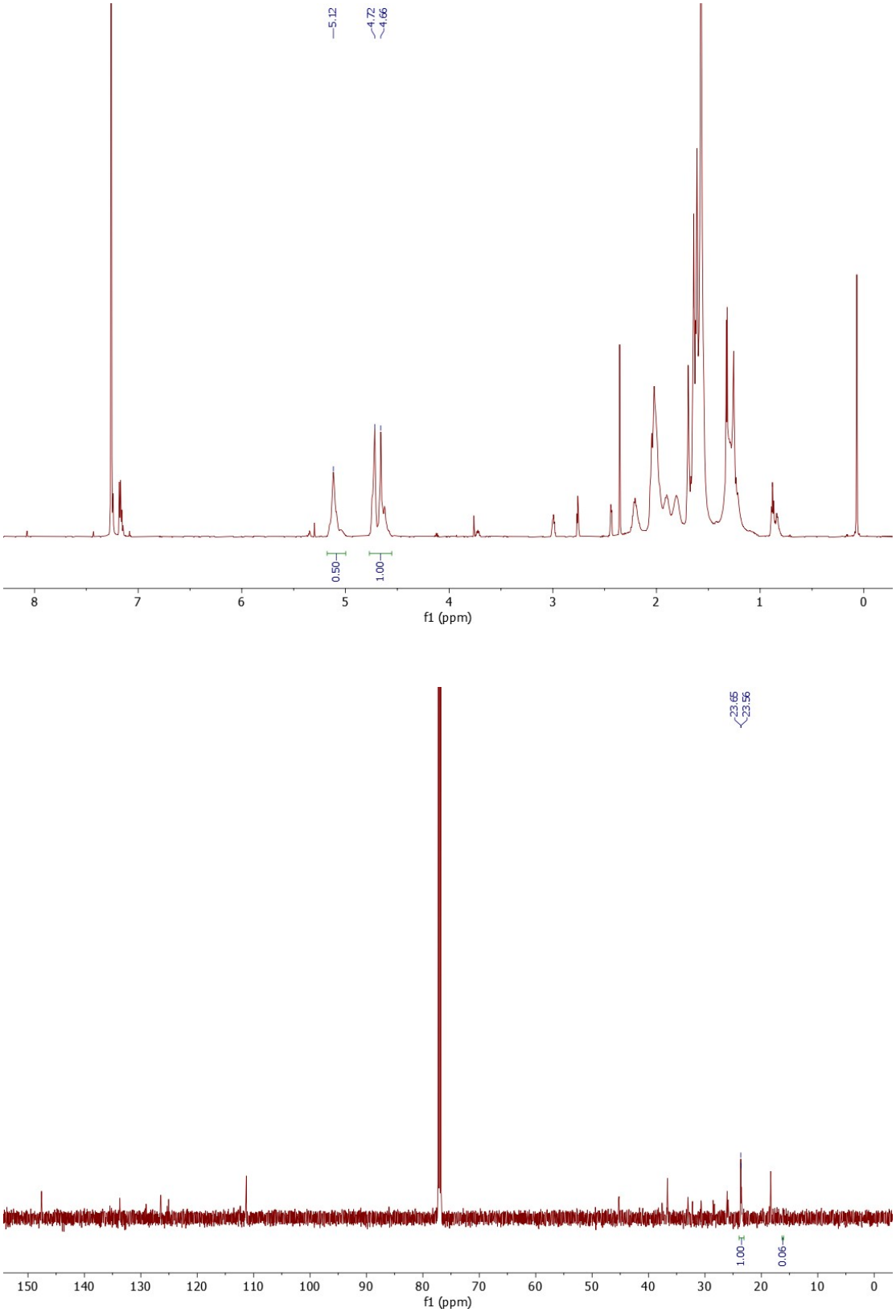

Figure S11. ^{1}H and ^{13}C NMR spectra of the polyisoprene obtained using **Fe^{H}**/MAO (Table 2, entry 12).

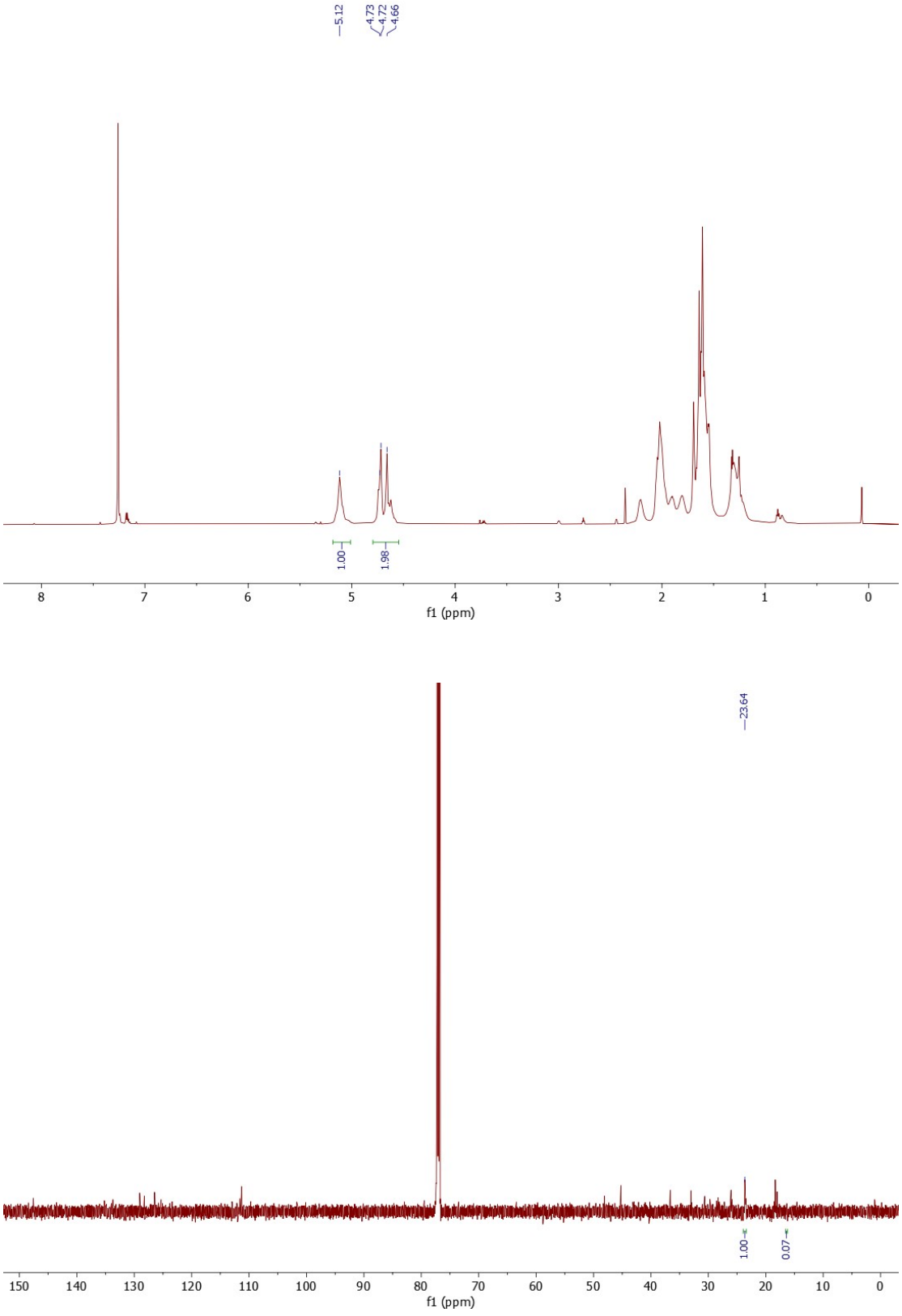

Figure S12. ^{1}H and ^{13}C NMR spectra of the polyisoprene obtained using **Fe^{H}**/MAO (Table 2, entry 13).

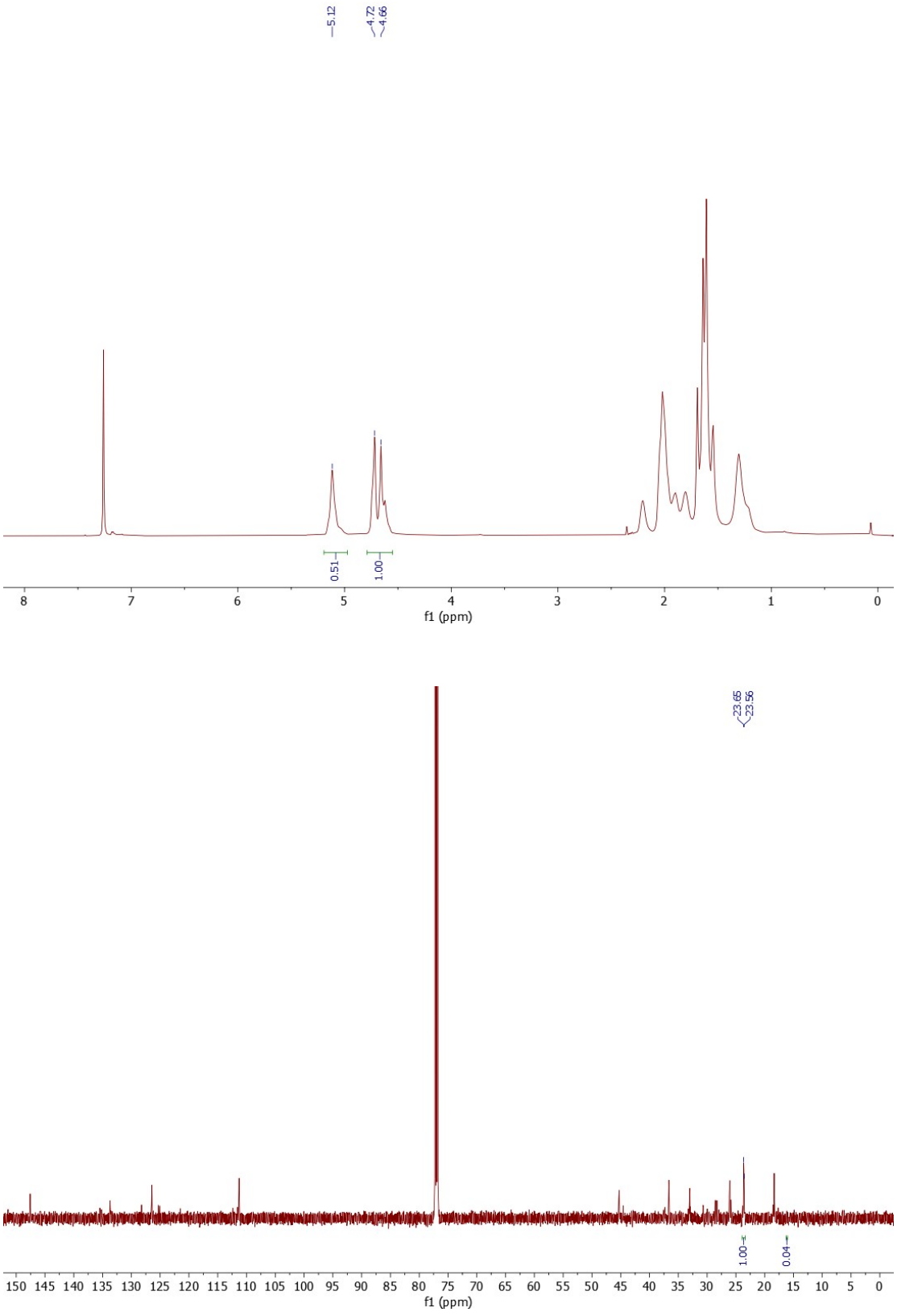

Figure S13. ^{1}H and ^{13}C NMR spectra of the polyisoprene obtained using **Fe^{H}**/MAO (Table 2, entry 14).

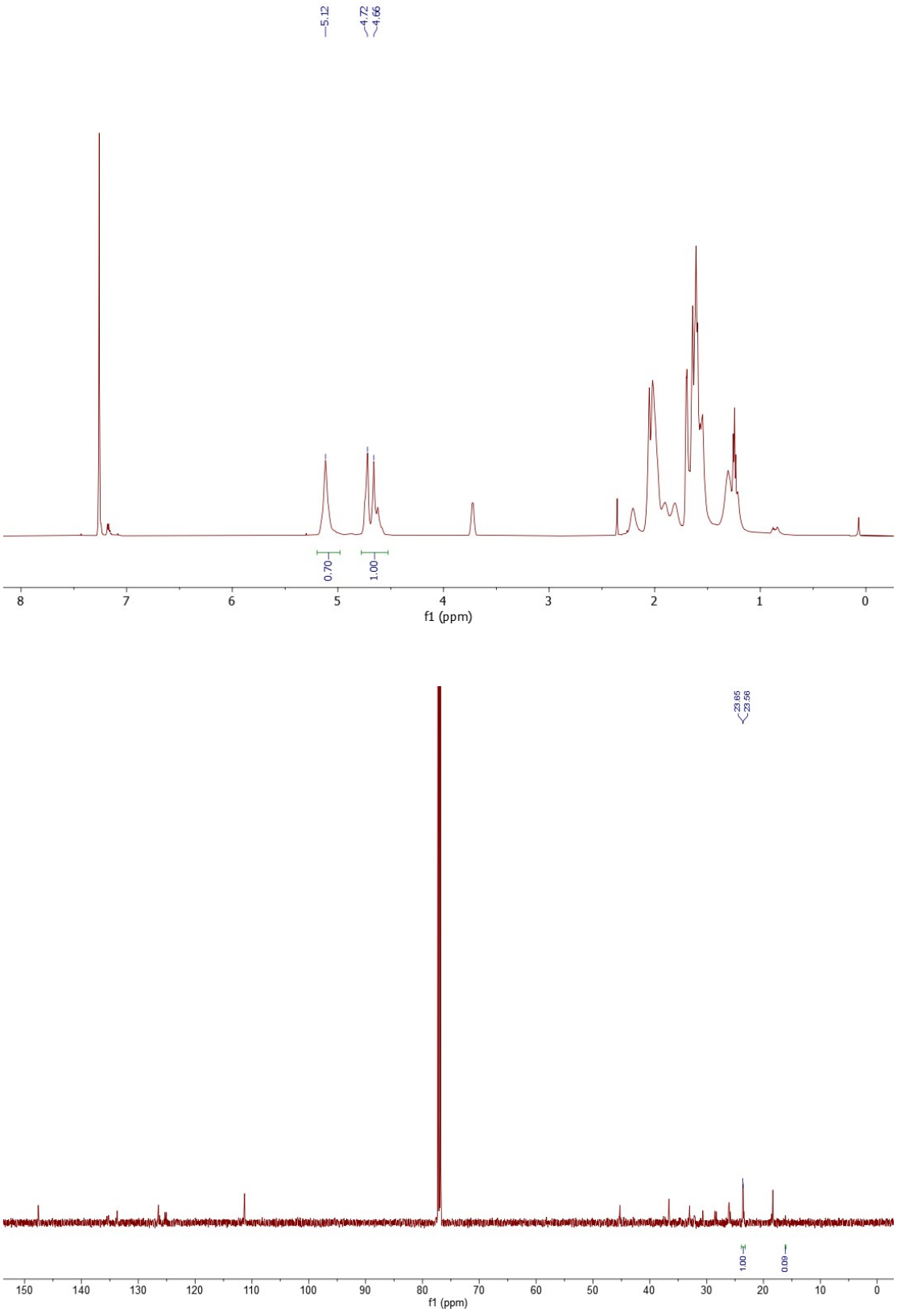

Figure S14. ^{1}H and ^{13}C NMR spectra of the polyisoprene obtained using **Fe^{2Me}**/MAO (Table 3, entry 2).

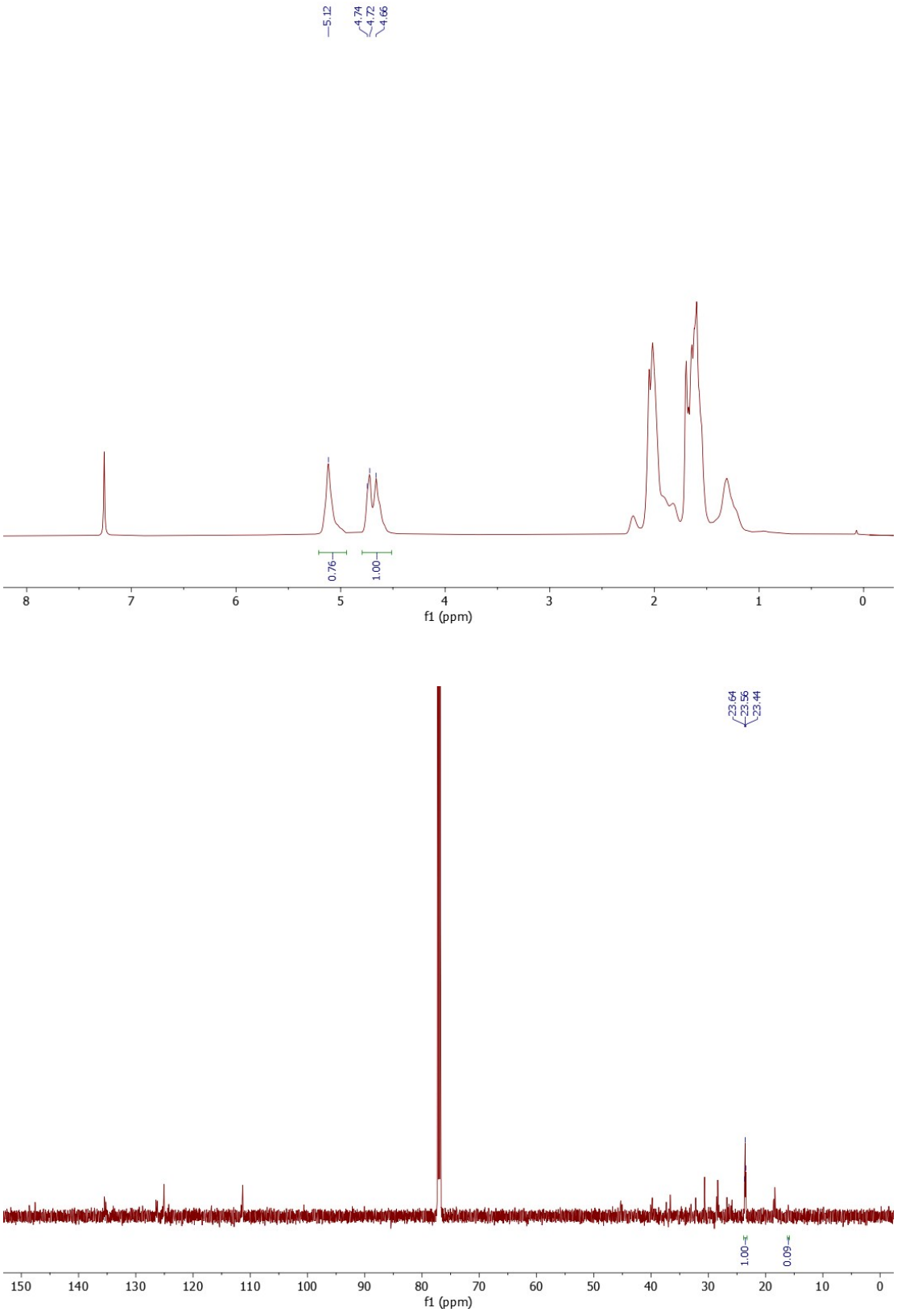

Figure S15. ^{1}H and ^{13}C NMR spectra of the polyisoprene obtained using **Fe^{2Et}**/MAO (Table 3, entry 3).

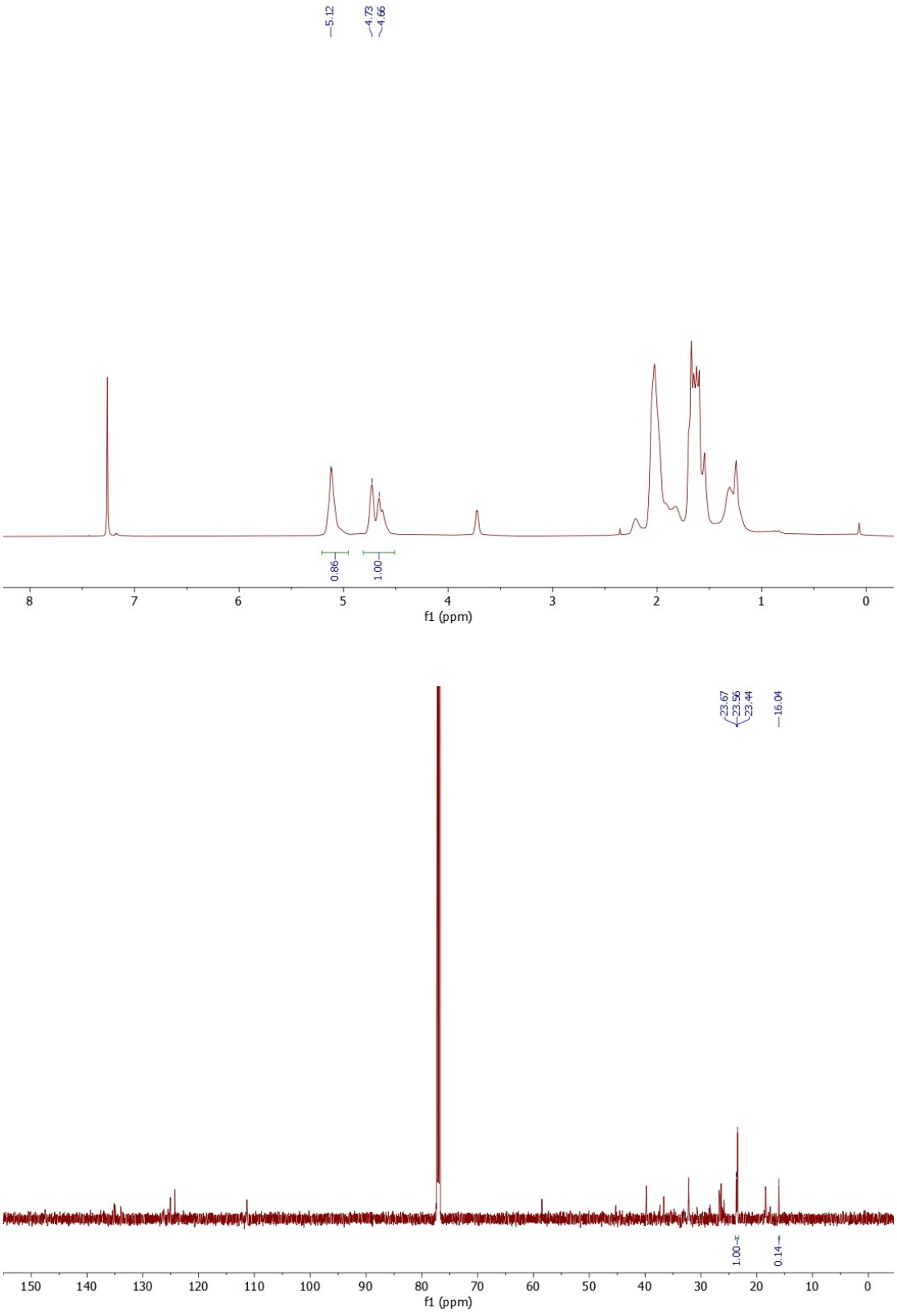

Figure S16. ^{1}H and ^{13}C NMR spectra of the polyisoprene obtained using **Fe^{2iPr}**/MAO (Table 3, entry 4).

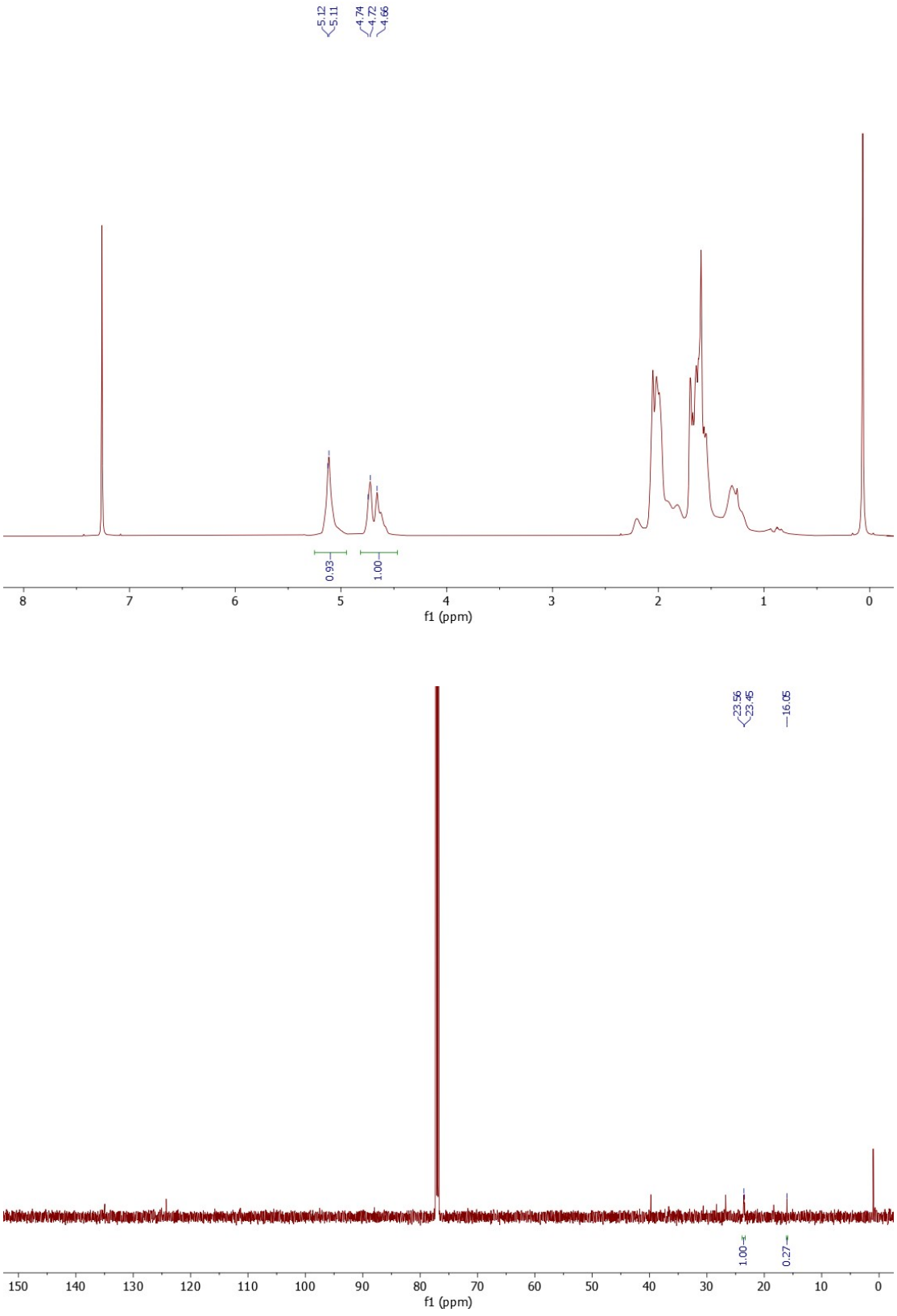

Figure S17. ^{1}H and ^{13}C NMR spectra of the polyisoprene obtained using **Fe^{3Me}**/MAO (Table 3, entry 5).

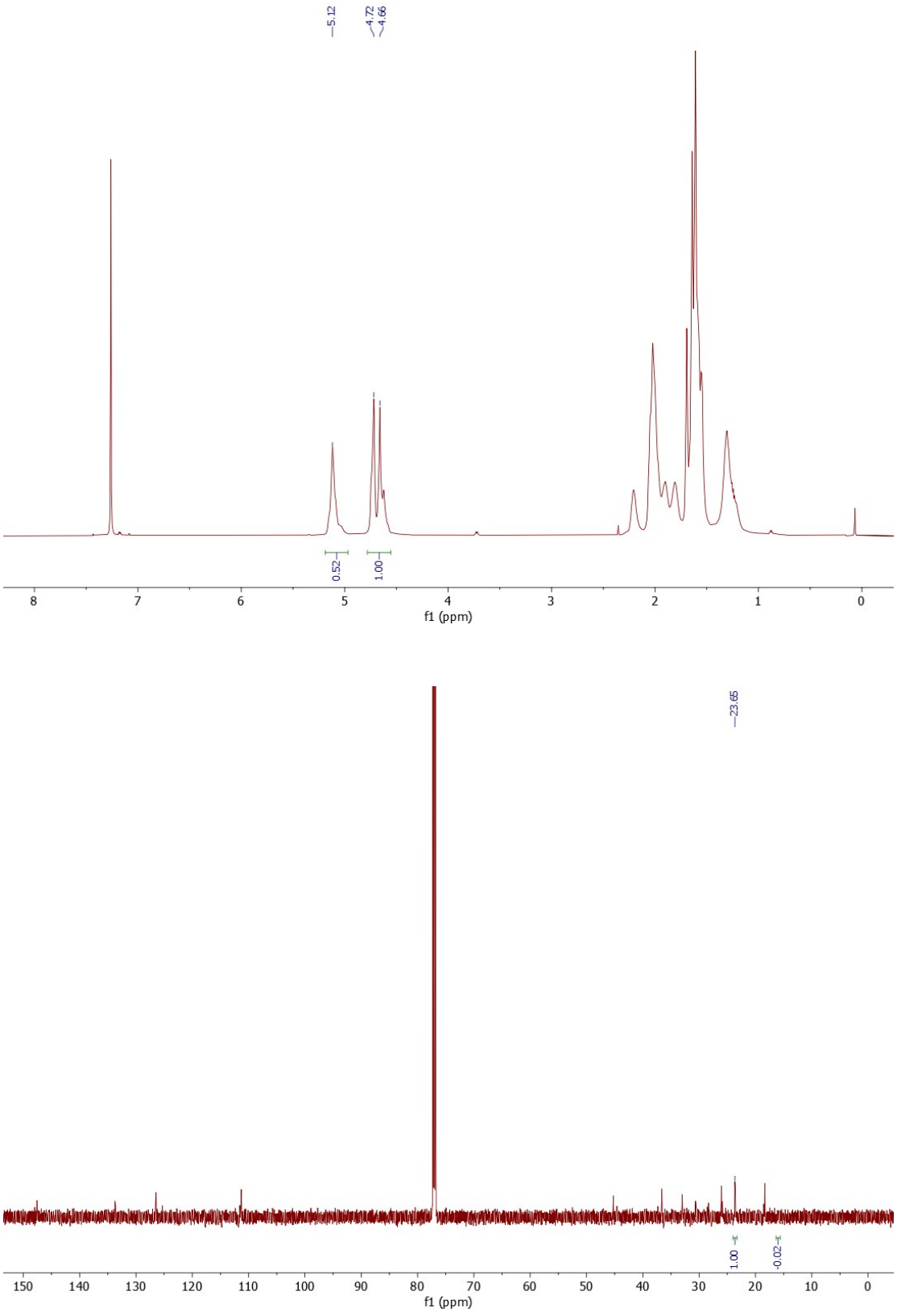

Figure S18. ^{1}H and ^{13}C NMR spectra of the polyisoprene obtained using $\mathbf{Fe^{H}}$/MAO (Table 4, entry 2).

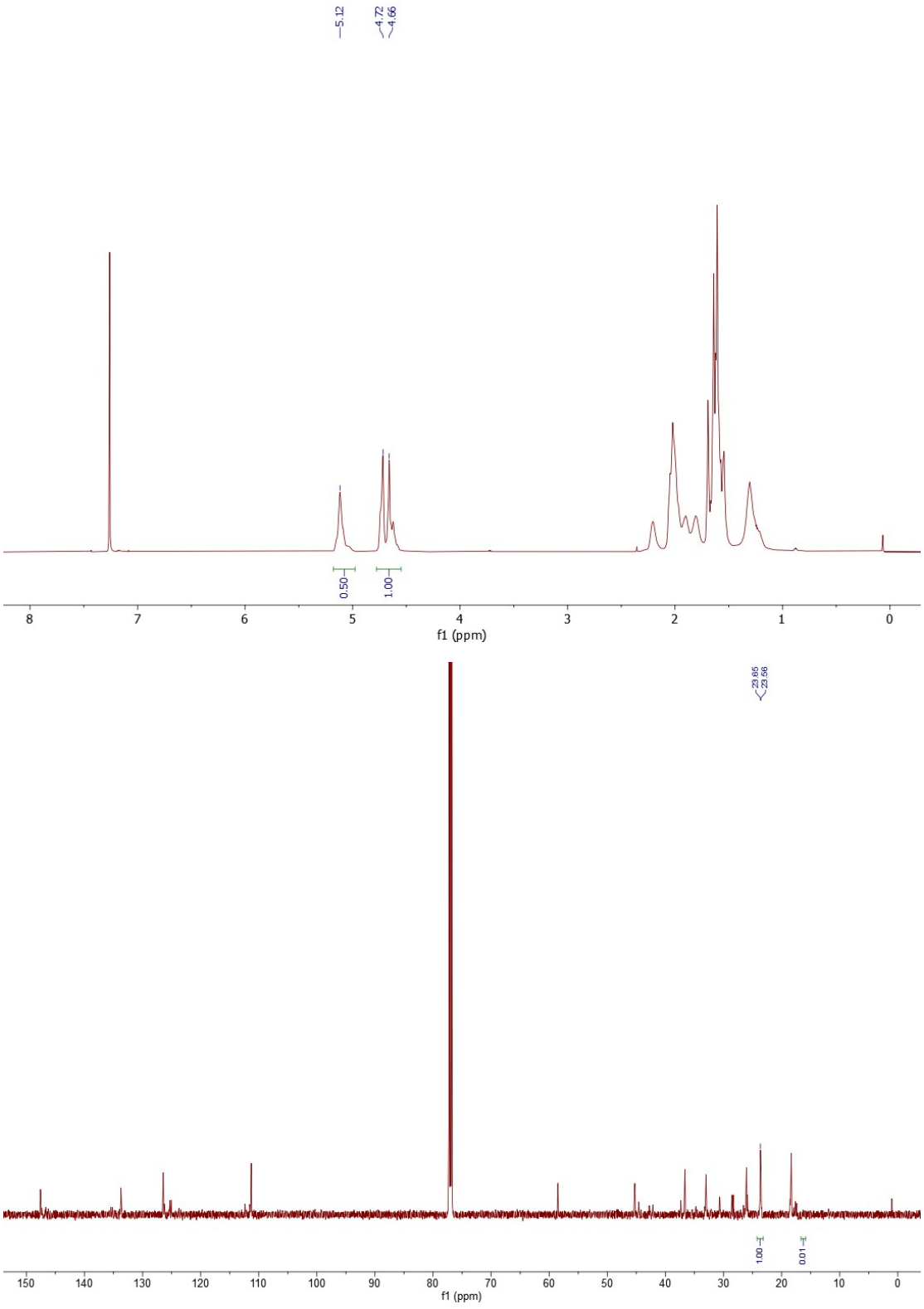

Figure S19. ^{1}H and ^{13}C NMR spectra of the polyisoprene obtained using $\mathbf{Fe^{H}}$/MAO (Table 4, entry 3).

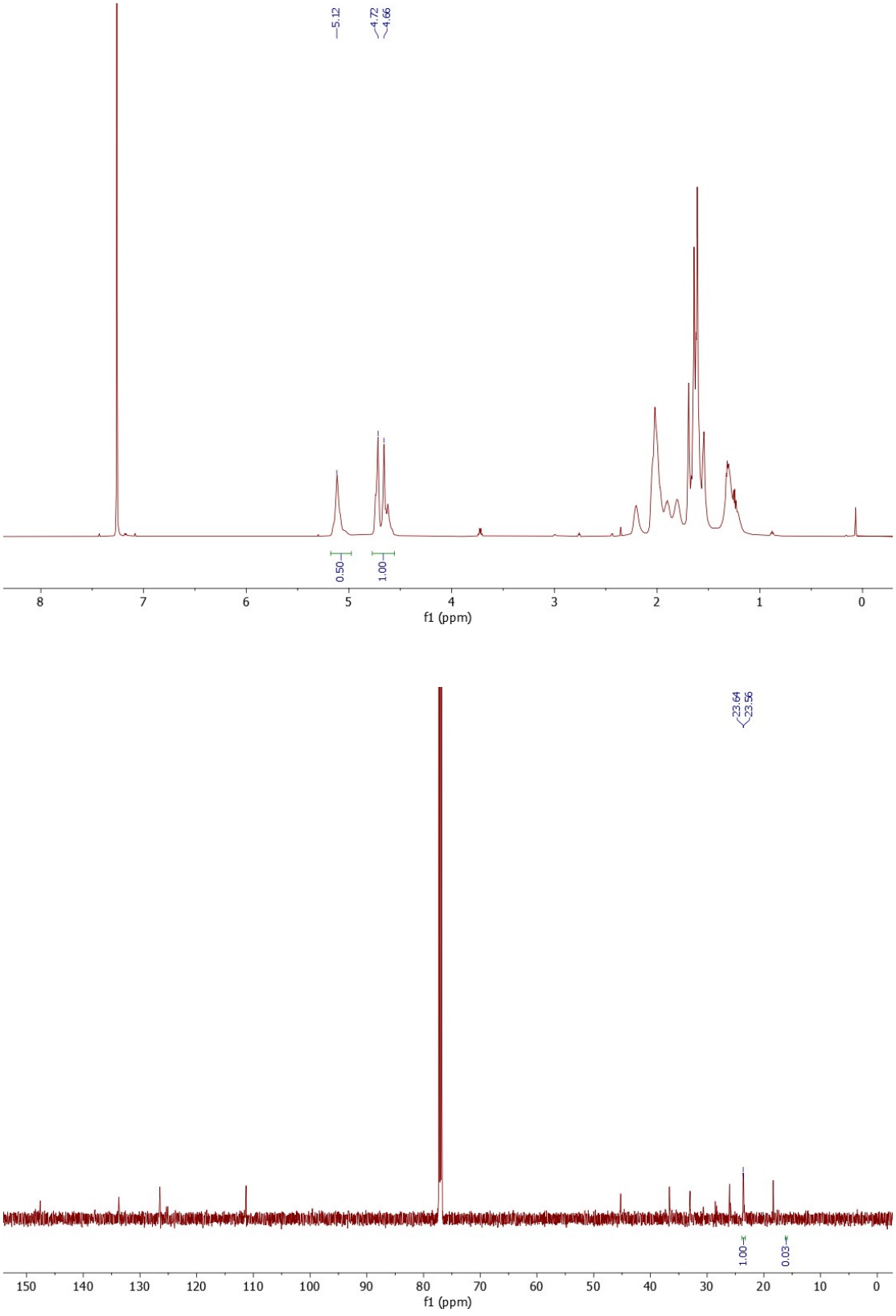

Figure S20. ^{1}H and ^{13}C NMR spectra of the polyisoprene obtained using **Fe^{H}**/MAO (Table 4, entry 4).

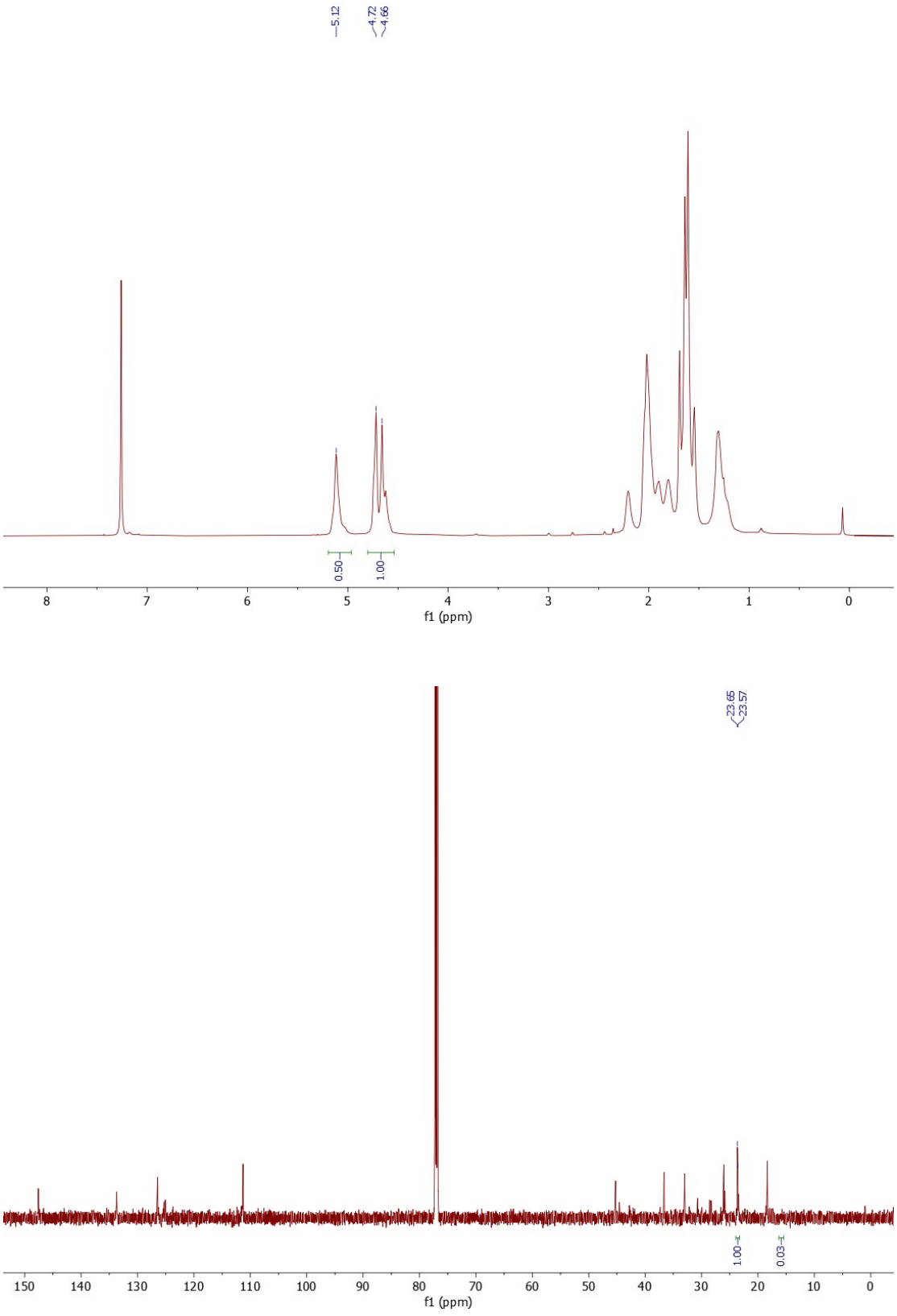

Figure S21. ^{1}H and ^{13}C NMR spectra of the polyisoprene obtained using **Fe^{H}**/MAO (Table 4, entry 5).

References

1. (a) G. M. Sheldrick, *Acta Crystallogr. Sect. A: Found. Adv*., 2015, **71**, 3–8; (b) G. M. Sheldrick, *Acta Crystallogr., Sect. C: Struct. Chem.,* 2015, **71**, 3–8; (d) O. V.

Dolomanov, L. J. Bourhis, R. J. Gildea, J. A. K. Howard and H. Puschmann, *J. Appl. Crystallogr.,* 2009, **42**, 339–341.